Microfluidic-based Bacterial Molecular Computing on a Chip

Daniel P. Martins, *Member, IEEE,* Michael Taynnan Barros, *Member, IEEE,* Benjamin J. O'Sullivan, Ian Seymour, Alan O'Riordan, Lee Coffey, Joseph B. Sweeney, and Sasitharan Balasubramaniam, *Senior Member, IEEE*

***Abstract*— Biocomputing systems based on engineered bacteria can lead to novel tools for environmental monitoring and detection of metabolic diseases. In this paper, we propose a Bacterial Molecular Computing on a Chip (BMCoC) using microfluidic and electrochemical sensing technologies. The computing can be flexibly integrated into the chip, but we focus on engineered bacterial AND Boolean logic gate and ON-OFF switch sensors that produces secondary signals to change the pH and dissolved oxygen concentrations. We present a prototype with experimental results that shows the electrochemical sensors can detect small pH and dissolved oxygen concentration changes created by the engineered bacterial populations' molecular signals. Additionally, we present a theoretical model analysis of the BMCoC computation reliability when subjected to unwanted effects, i.e., molecular signal delays and noise, and electrochemical sensors threshold settings that are based on either standard or blind detectors. Our numerical analysis found that the variations in the production delay and the molecular output signal concentration can impact on the computation reliability for the AND logic gate and ON-OFF switch. The molecular communications of synthetic engineered cells for logic gates integrated with sensing systems can lead to a new breed of biochips that can be used for numerous diagnostic applications.**

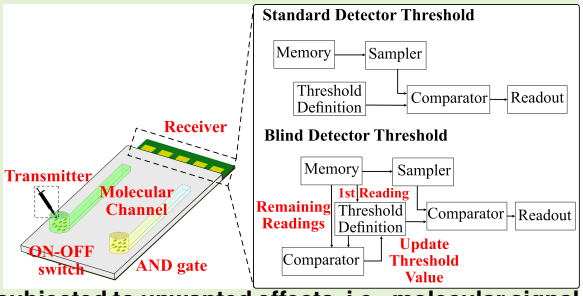

***Index Terms*— Bacterial molecular computing, Biosensors, Electrochemical sensing, Microfluidics , Molecular Communications, Synthetic logic gates.**

I. Introduction

BIOCOMPUTING is an emerging research field that envisions the use of biological componets to create computing tasks in the very same way that silicon technology is used today in conventional computing devices [1]. These systems can be based on prokaryotic cells, such as bacteria, and can be used for example applications such as detection of metal ions, as well as controlled communication functionalities through emission of signalling molecules [2]–[5]. Biocomputing systems can be integrated into molecular computing chips, where they can be used as biosensors to diagnose and analyse biological samples and specimen. The computing function can be achieved through the communications within a bacterial population, through the engineering of their natural communications system [5], [6], (i.e., *quorum sensing* signalling), which leads to the production, emission and reception of molecules used by microbes to coordinate their collective behaviour in both small and large populations [7].

Bacteria signalling processes have been used in the design of engineered nanoscale biological systems for performing logic computations [8]–[11]. Such engineered signalling processes can tune the computing operation accuracy and this builds on a new communications theory paradigm known as **Molecular Communications (MC)** [4], [11]–[17]. The characterization and design of artificial communication systems built from biological components found in nature is the main goal for Molecular Communications systems. However, the development of an operational molecular computing system for diagnostics will require other accompanying technologies, such as translation from chemical into electrical signals. An example of this technology, considered in this paper, is electrochemical-

Submitted on March 2022. Resubmitted on April and June 2022. This work was funded by Science Foundation Ireland and the Department of Agriculture, Food, and Marine via the VistaMilk research centre (grant no. 16/RC/3835).

Daniel P. Martins is with the Walton Institute for Information and Communication Systems Science, South East Technological University Waterford West Campus, Carriganore, Ireland, X91 P20H. E-mail: daniel.martins@waltoninstitute.ie.

Michael Taynnan Barros is with the University of Essex, Colchester, United Kingdom, CO4 3SQ, and with the Computational Biophysics and Imaging Group, BioMediTech, Faculty of Medicine and Health Technology, Tampere University, FI-33014 Tampere, Finland. Email: m.barros@essex.ac.uk

Benjamin O'Sullivan, Ian Seymour and Alan O'Riordan are with Tyndall National Institute, Cork, Ireland, T12 R5CP. E-mail:{benjamin.osullivan, ian.seymour, alan.oriordan}@tyndall.ie

Lee Coffey is with the Pharmaceutical & Molecular Biotechnology Research Centre, South East Technological University Waterford, Cork Road, Waterford, Ireland, X91 K0EK. E-mail: lee.coffey@setu.ie

Joseph Sweeney is with the LIFE farm4more, University College Dublin, Dublin, Ireland. E-mail: joseph.sweeney@ucd.ie

Sasitharan Balasubramaniam is with the School of Computing, University of Nebraska-Lincoln, 104 Schorr Center, 1100 T Street, Lincoln, NE, 68588-0150, USA. E-mail:sasi@unl.edu

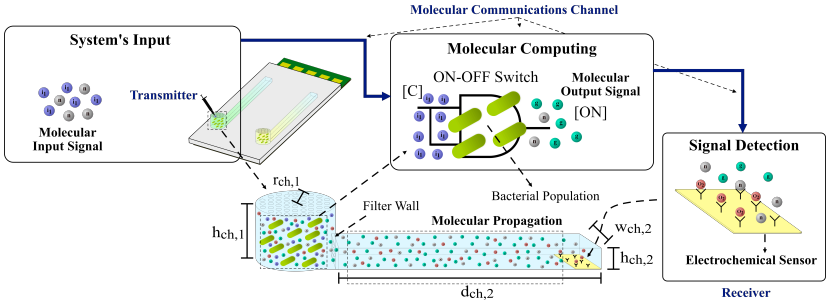

Fig. 1. Illustration of the proposed microfluidic-based bacterial molecular computing on a chip, focused on one of its microfluidic structures. The proposed system utilises engineered bacteria populations, configured as an ON-OFF switch and AND logic gate, to compute molecular signals (coloured spheres). Here, the blue, gray, green and red spheres represent the molecular input signal, the molecular noise, the molecular output signal and the oxygen concentration, respectively. The measurement of dissolved oxygen concentration is done using an electrochemical sensor, which use different estimation strategies to improve the detection of molecular signals (please refer to Section V for further details).

based sensing. However, interfacing biocomputing cells to electrochemical sensing systems can lead to challenges that includes obtaining precise readings of the noisy biologically computed molecular signals [18]–[20]. To that end, here we propose a bacteria-based biocomputing system and design a method for the accurate detection of molecular signals emitted by it. Based on that, we evaluate the end-to-end reliability of the proposed biocomputing system within a biochip.

Biochips based on microfluidics (a.k.a, lab-on-chip) have been extensively reported in the literature, specially for the drug discovery and *in situ* diagnostics. These devices are portable and easy-to-use platforms for the analysis of biomolecules and are driving the innovation in the fields of life sciences, and biochemistry [8], [21]–[26]. Inspired by these works, we introduce the concept of *Microfluidic-based Bacterial Molecular Computing on a Chip (BMCoC)*, which integrates electrochemical sensors and bacteria-based molecular computing systems by analyzing and estimating the molecular communication through signal detection theory.

Our proposed solution differs from the current lab-on-chip devices due to the molecular signal detection and computing using an AND Boolean logic gate and an ON-OFF switch sensors that is constructed from engineered bacterial populations (see Figure 1) [27], [28]. Here, the engineered bacterial populations detect and compute molecules in the environment outside of the microfluidic device (hereinafter named as molecular input signal), resulting in new molecules that affect the pH and dissolved oxygen levels inside of the microfluidic structure (hereinafter named as molecular output signal). As shown in Figure 1, the electrochemical sensors are used to quantify the variation of dissolved oxygen levels and indirectly measure the molecular output signal concentration (a similar process is done to measure the pH level within the microfluidic chip). We utilise this measurement to assess the reliable logic computation (RLC) probability of our chip, i.e., the probability of correct computation results in a logical "0" or "1" at the electrochemical sensors, which can be affected by unwanted effects such as delays (caused by the process of insertion of molecules into the chip and due to media and microfluidic tube structure) and resulting in the reduction of the chip's computing performance. These unwanted effects are further described in Sections III and IV. Here we use a similar electrochemical sensing system design as in [8] to measure the pH and the dissolved oxygen concentration change due to the emission of molecular signals from the engineered bacterial population. Nevertheless, as we are interested in reliably detecting molecular output signals at the receiver (i.e., correct detection of bits "0" and "1"), we also propose two estimation techniques to provide some intelligence to the electrochemical sensors and improve the system's performance (please refer to Section V for further details). These techniques focus on the selection of an appropriate detection threshold value to improve the determination of the logical values of "0" and "1" to the detected molecular output signal concentrations. Please note that similar procedures can also be found in conventional electronic systems [29]. Moreover, our suggested application improves on the design proposed by [30] as it considers lesser moving parts and relies on free-diffusion to transport the molecular information. For our proposed system, the engineered bacterial populations receive chemicals to produce and emit molecular signals through a microfluidic channel that gets propagated towards an electrochemical sensors to detect the output from the computing operation. Our main contributions are as follows:

- **Analysis of the BMCoC components through laboratory experiments:** The engineering of the bacterial populations and the electrochemical sensors are introduced, and microbiology assays and electrochemical experiments are performed to describe the performance of these main components of the BMCoC design.
- **A communication system model for the analysis of the BMCoC performance:** We propose the use of multiple engineered bacterial populations to compute different molecular input signals and perform a theoretical analysis of the communications processes, focusing on the detection of the molecular output signal, which can affect the performance of the BMCoC.
- **Analysing the reliability of molecular environmental signals computation:** We analyse the impact of two factors, production delay and molecular input signal concentration, on the correct detection of molecular output signal by the electrochemical sensors, which we defined as reliable logic computation probability.

In the next section we introduce and provide an overview

of BMCoC. In Section III, we describe the physical design of the BMCoC. Then, in Section IV we present the molecular communications model for the BMCoC, which supports the signal detection estimation and computing reliability introduced in Section V. Next, in Section VI we present our experimental results for molecular computing by the bacterial population, and the results obtained for the analysis of the BMCoC reliability logic computation for varying delays and molecular input signal concentrations. Lastly, in Section VII we present our conclusions.

II. Overview of the BMCoC

BMCoC is a device that transduces the molecular signals computed by engineered bacteria into electrical current or potential and can be connected to a wireless interface, enabling its remote monitoring. The BMCoC contain a number of microfluidic tubes that will store and interconnect the engineered bacteria with the electrochemical sensors, which are placed on a printed circuit board. Figure 1 illustrates the molecular communications system proposed to support the operation of the BMCoC within microfluidic tubes and can be divided into two chambers: one that stores the engineered bacteria and the second tube where the molecules emitted by the bacterial population are diffused (see Section III for more details). For the proposed device, the molecular input signals are computed by each bacterial population resulting in a secondary signal that is diffused towards the electrochemical sensor.

To process the molecular input signals placed on the BMCoC surface, the bacteria are engineered to act as logic gates (AND gate and ON-OFF switch), and the molecular output signal produced by these bacterial populations modifies the pH of the fluid media or the dissolved oxygen concentration in the microfluidic tube. Figure 1 illustrates how the BMCoC receives, processes and detects the molecular signals. The whole process starts with the insertion of the molecular input signals that will diffuse towards the engineered bacteria and produces output secondary molecular signal that will be diffused through the microfluidic tube and detected by the electrochemical sensor. The detection process is performed by electrochemical sensors that can utilize different estimation techniques depending of the context of the BMCoC application, and they are implemented as a post-processing step for our system. When all the system's characteristics are known *a priori*, the electrochemical sensor circuit board implements a standard detector threshold. An alternative technique is based on the blind detector threshold that can be implemented to increase the reliability of the system. Please note that, while in the following section we further detail the physical design of the BMCoC, the detailed experimental methodology is described in the Appendix I and II.

III. Physical Design of the BMCoC

In this section, we introduce the physical design of the BMCoC's main components: a microfluidic structure that encase the bacterial populations and serves as the waveguide for the molecules produced by them, and the custom-made electrochemical sensors chip that will detect the pH and dissolved oxygen variation around the electrodes.

A. Microfluidic Tube Structure

The design of the microfluidic tube follows a similar approach to [24], [31], where polydimethylsiloxane (PMDS) is used. As mentioned in Section II, the microfluidic tube is divided into two chambers. One chamber is shorter than the other and stores the bacterial population with a volume of $V_{ch,1} = \pi r_{ch,1}^2 h_{ch,1}$, where $r_{ch,1}$ and $h_{ch,1}$ are the radius and the height of the microfluidic chamber, respectively. The longer microfluidic chamber is designed to allow the free diffusion of the molecular output signal emitted by the bacterial population, and its volume is given by $V_{ch,2} = d_{ch,2} h_{ch,2} w_{ch,2}$, where $h_{ch,2}$, $d_{ch,2}$ and $w_{ch,2}$ are the height, length and width of the chamber. The dimensions of each microfluidic tube are defined with respect to the desired applications. The two chambers that make up the tube are interconnected by an encapsulating porous membrane that allows the molecules to flow through the tube and not the bacterial cells [11], [32].

B. Electrochemical Sensor

The electrochemical sensors chip situated at the bottom of the tube is composed by gold interdigitated electrodes (two combs), platinum pseudo reference and gold counter electrodes. The chip also includes a microSD port to interface the electrodes with external electronic devices [31], [33], [34]. The interdigitated microband structure of the combs is fabricated using blanket metal evaporations of titanium and gold (10 nm and 100 nm, respectively) and a lift-off technique. To evaporate these two metals, a Temescal FC-2000 E-beam machine was used, and the resulting microband structure (55 μm x 1 μm x 60 nm) have gaps between combs of 1, 2 and 10 μm. To fabricate the gold counter (that have the following dimensions 90 μm x 7 mm) and the interconnections required for the operation of the electrochemical sensor, we repeat the process applied to the interdigitated microband structure (no titanium is used in this step). Finally, we performed a third metal evaporation to create the platinum pseudo-reference electrode responsible for the detection of the current magnitudes. To avoid issues caused by any reading inconsistencies during the development phase of the pseudo-reference electrode, we utilize an external reference electrode. Moreover, we insulate the connection tracks by performing a plasma-enhanced chemical vapour deposition of silicon nitride. The electrolyte only access these tracks through small windows (45 μm x 100 μm) selectively created in the insulating layer. A similar procedure was done to create openings over the remaining components of the electrochemical sensor.

We also fabricated a holder cell to measure the small electrolyte volumes utilized in our experiments (from 50 μL to 5 mL). The base of this structure is made using aluminium while its lid uses Teflon to isolate the spring-loaded probes that crosses it (they are positioned above the peripheral contact pads) to create a connection for external potentiostast. Then we sealed the on-chip electrodes using Viton O-rings, which possess the chemical resistance required for our experiments, and assemble the whole structure. Please note the chosen Viton O-rings have the required dimensions (inner diameter of 7

This article has been accepted for publication in IEEE Sensors Journal. This is the author's version which has not been fully edited and
content may change prior to final publication. Citation information: DOI 10.1109/JSEN.2022.3192511

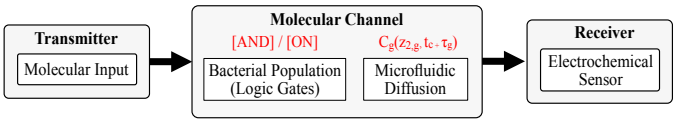

Fig. 2. Representation of the bacteria-based molecular communications system that supports the operation of the engineered bacterial population logic computing.

mm and a cross-section of 1.6 mm) to seal the electrodes, while exposing the sensors, counter and reference electrodes to the electrolyte. For our setup, the electrochemical sensors can detect from pH 14 to 0, or 10^{-14} to 0 molecules (respectively), and dissolved oxygen from 0.5 ppm to 9 ppm. These values enable us to perform the experiments without sensitivity issues. In case of sensing scenarios that falls outside of the current BMCoC design, a simple replacement of the electrochemical sensor (with increased sensitivity) would be sufficient.

IV. MC Model of the BMCoC

In this paper, we model the different components of the BMCoC using molecular communications theory, and the represented communications model is illustrated in Figure 2. For this model, we are especially interested in describing the insertion, processing and detection of molecules. Therefore, in this section we introduce and describe each one of the components of our molecular communications system.

A. Transmitter

Transmitters are responsible to prepare the information signal to be sent through the communications channel. In our model, the transmitters represent the pipette (used in our wet lab experiments) or any other instrument/device used to insert molecules into the microfluidic system containing the engineered bacterial population. Here, we consider that the molecular input signals are pipetted into the microfluidic chamber like a train of pulses with amplitude m_i and this signal reaches the engineered bacterial populations to activate their computing process. This step of our model is defined as follows [35]

$$[A] = [B] = [C] = \frac{m_i s_i}{\sqrt{4\pi D(t_c + \tau_{in})}} e^{\frac{-z_{1,g}^2}{4D(t_c+\tau_{in})}} \quad (1)$$

where s_i is the train of pulses function generated by the insertion of the molecules in the BMCoC, m_i is the concentration (pulse amplitude) of the molecular input signals, $z_{1,g}$ is the Euclidean distance from the insertion point and the centre of the bacterial population; τ_{in} is the propagation delay between insertion point and the bacterial population, $i = \{A, B, C\}$ is the representation of the three molecular input signals considered for the operation of the AND gate and ON-OFF switch, $g = \{AND, ON\}$ identifies the logic computation process, and t_c is the duration of the molecular signal's insertion into the bacterial population's chamber. Please note that (1) is a general model to represent the insertion of molecules in the microfluidic system. However, in our experimental setup we utilise nitrile and IPTG for the AND gate (signals A and B respectively), as well as acetate or propionate for the ON-OFF switch, i.e., signal C (see Appendix I for more details). Please also note, this equation combines the transmission of molecules (which can be modelled using [11, eq. (6)]) with the solution of Fick's diffusion equation [35], and the molecular concentrations of each one of the three inputs, considered in this work, will activate the logic computing process in the engineered bacterial populations.

B. Channel

Bacteria can process molecular signals as switches, amplifiers, or logic gates [11], [36]. As a result from this internal process, the bacteria produces the molecular output signal that drive their individual and collective behaviours. Here we the communication channel is composed of both the bacterial internal processing of molecules and the propagation of the molecular output signal.

Biologically, bacteria process molecules using a series of chemical reactions, namely signalling pathways, which result in new molecules that are used in a wide variety of behaviours, such as movement, energy production and reaction to stress [37]. Therefore, to model such chemical reactions, we use differential equations that represent the molecular concentration change over time for the both AND gate and the ON-OFF switch operations. While the ON-OFF switch operates using a single molecular concentration to produce the molecular output signal (affecting the dissolved oxygen concentration around the electrochemical sensors), the AND gate requires two molecular input signals to modify the pH of the fluid inside of the microfluidic chamber of BMCoC. Therefore, the AND gate and the ON-OFF switch processes are represented as follows

$$\frac{d[x_{AND}]}{dt} = \frac{[A]^n}{K_A^n + [A]^n} \cdot \frac{[B]^n}{K_B^n + [B]^n} - \gamma[x_{AND}] + N_{x_{AND}}(t) \quad (2)$$

$$\frac{d[x_{ON}]}{dt} = \frac{([C]^n)^2}{(K_C^n)^2 + 2K_C^n[C]^n + ([C]^n)^2} - \gamma[x_{ON}] + N_{x_{ON}}(t), \quad (3)$$

where x_{AND} and x_{ON} are the molecular output signals from the AND gate and ON-OFF switch, respectively; K_A, K_B and K_C are the equilibirum constants for the signals $[A]$, $[B]$ and $[C]$, and express the relationship between the molecules involved in the chemical reaction at equilibrium; γ is the rate that the molecular output signal is naturally degraded in the environment; n is the Hill coefficient and measure of the cooperativity in these chemical reactions (for more details on these chemical parameters see [38]), t is total duration of the computing process, and $N_{x_{AND}}(t)$ and $N_{x_{ON}}(t)$ is the fluctuation of the molecular signal production which is modelled as an Additive White Gaussian Noise (AWGN) for these molecular output signals (see [11] for a further explanation about this assumption).

The molecules produced by each engineered bacterial population will travel through the microfluidic tube independently.

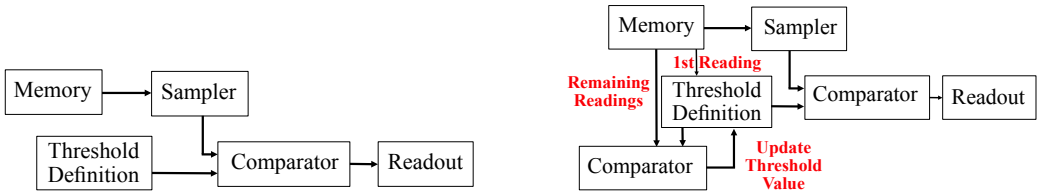

Fig. 3. Representation of the estimation techniques considered in this paper. (a) The standard detector threshold can be applied when the electrochemical sensors know *a priori* the conditions the molecular output signal is subjected to. (b) When not knowing the concentration changes due to unwanted effects and conditions, the electrochemical sensor might apply the blind detector threshold.

Therefore, this propagation channel $C_g(z_{2,g},t)$ can be characterised using the solution for the Fick's diffusion equation, and represented as follows [35]

$$C_g(z_{2,g},t) = \frac{1}{\sqrt{4\pi Dt}} e^{\frac{-z_{2,g}^2}{4Dt}}, \tag{4}$$

where D is the diffusion coefficient for the propagation of the molecular signals in the fluid channels, $z_{2,g}$ is the Euclidean distance between the engineered bacterial gates centre and the electrochemical sensor. Please note that the time t includes all the delays considered in this process, including τ_g, which is the propagation delay between the bacterial population and the electrochemical sensor. Moreover, our distance assumption ensures that each bacterium will equally contribute to the molecular computation. This model also assume that the molecules dimensions are much smaller than the microfluidic tubes dimensions, allowing us to model the channel using a solution for Fick's diffusion equation.

C. Receiver

Here we consider the electrochemical sensors as the receiver in our molecular communications model. The molecular output signal after being transmitted through the propagation channel $C_g(z_{2,g},t)$ results in the molecular signal $y_g(z_{2,g},t)$ that reach the region where the receiver is able to detect the changes in pH or the dissolved oxygen concentration. The molecular signal $y_g(z_{2,g},t)$ can be evaluated as follows

$$y_g(z_{2,g},t) = [x_g] * C_g(z_{2,g},t) + n_g(z_{2,g},t), \tag{5}$$

where $*$ denotes the convolution operation, $[x_g]$ is the molecular output signal produced by the AND gate and ON-OFF switch ($g = AND$ and $g = ON$, respectively), which is evaluated using (2) and (3), and $n_g(t)$ is the electrolyte noise. As this system is confined by the microfluidic structure, and the engineered bacterial population would only emit the molecules of interest, the detection of the molecular output signal is only affected by the electrolyte noise, which is produced by the resistance due to the passage of the molecular signal on the electrochemical sensors and is defined as [39]

$$n_g(z_{2,g},t) = 4kTR_b(z_{2,g},t), \tag{6}$$

where $R_b(z_{2,g},t) = \frac{1}{\Gamma(z_{2,g},t)}\sqrt{\frac{\pi}{a_e}}$ is the electrolyte resistance, $\Gamma(z_{2,g},t) = \Gamma_s y_g(z_{2,g},t) \times 10^3$ is the conductivity of the molecular signal [38], k is the Boltzmann constant, T is the absolute temperature, and a_e is the passage area of the electrochemical sensors.

V. Reliability Analysis of Logic Computation

Existing channel properties affect the signals that reach the electrochemical sensors, including delays and noise, and impact on the quality and capacity of a molecular communications system [11], [19], [40]. Therefore, we consider two signal reception estimation techniques (standard and blind detector thresholds) to ensure that the electrochemical sensors is able to detect lower levels of molecular signals and their respective concentration values. Our goal is to verify whether these estimation techniques can improve the reliability of the logic computation.

A. Standard Detector Threshold

We first consider the case where the electrochemical sensors do know *a priori* the conditions that the molecular output signal might be subjected to, such as the characteristics of the microfluidic tube, the engineered bacterial population behaviour, and the system inputs. In this case, a fixed detection value (hereinafter named as standard detector threshold), $r_{std,g}$, is defined based on the molecular output signal concentration that the engineered bacteria will diffuse through the microfluidic tube (see Figure 3a). This is defined as follows

$$\hat{r}_{std,g} = \frac{\max(y_g(z_{2,g},t))}{2}, \text{ for } \quad 0 \leq t \leq t_{p=1}, \tag{7}$$

where $p = 1, ..., p_{tot}$ is the pulse index, p_{tot} is the total number of pulses, and t_p is the period of each pulse.

B. Blind Detector Threshold

In the case where the electrochemical sensors do not know *a priori* the conditions that the molecular output signal is subjected to, a dynamic detection value assignment (hereinafter known as blind detector threshold) should be applied (see Figure 3b) [41]. The BMCoC device will continuously read the pH or the dissolved oxygen concentration change and store information for *a posteriori* detection. The proposed estimator, inspired by [41], consists of two steps. First, the electrochemical sensor will measure the maximum molecular output signal concentration, produced for a short period, L_p. Then the initial detection threshold value, $\hat{r}_{u,g,p}$, is defined as follows

$$\hat{r}_{1,g,1} = \frac{\max(y_g(z_{2,g},t_{p=1}))}{L}, \tag{8}$$

where u and p are the threshold and the pulse index, and they are equal to 1 in this case; and $L = 10$ seconds is the measuring period for the molecular concentration reaching the

This article has been accepted for publication in IEEE Sensors Journal. This is the author's version which has not been fully edited and content may change prior to final publication. Citation information: DOI 10.1109/JSEN.2022.3192511

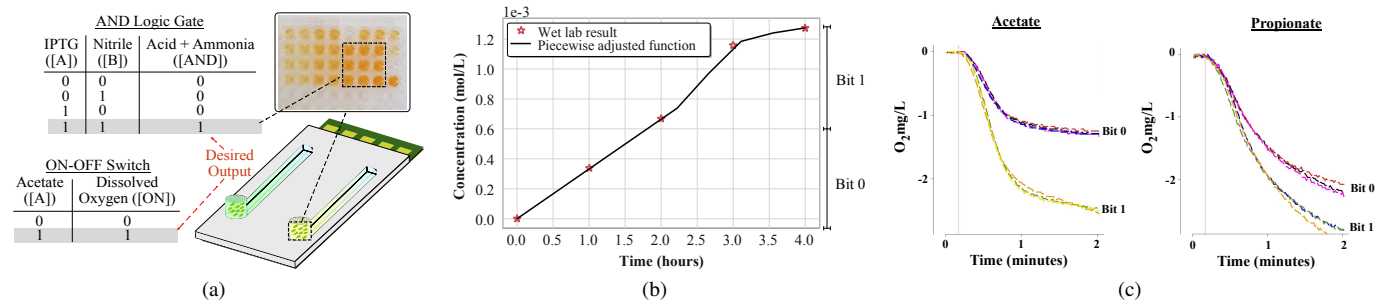

Fig. 4. Illustration of the wetlab experiments performed to investigate the performance of the bacterial populations. (a) A 96-well plate assay was performed for the synchronized production of the molecular signal by the AND gate. (b) Linear fitting of the molecular concentration produced by the bacterial population is shown for the desired output of the AND gate. c) Plot results for the acetate and propionate exclusion ON-OFF switches operation. The dashed red line represents the respective biosensors insertion delay. For the acetate case, the ON-OFF switch shows a O_2 consumption response for $\mathbf{0.2}$ mmol/l and $\mathbf{0.4}$ mmol/l molecular input (bit "0" and bit "1", respectively), while the propionate ON-OFF switch shows its O_2 consumption responses for $\mathbf{0.16}$ mmol/l and $\mathbf{0.21}$ mmol/l (bit "0" and bit "1", respectively).

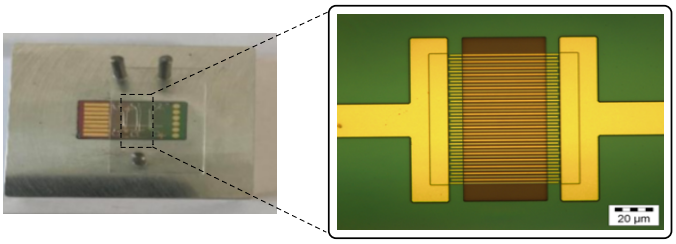

Fig. 5. Image taken of the microfluidic channel and electrodes considered in this paper. We magnified ($\mathbf{50x}$) a section of the microfluidic channel to visualise the gold IDE array used for both pH measurements and oxygen quantification.

receiver. Second, the electrochemical sensor will continue to measure the molecular output signal concentration to improve the detection threshold. In this stage, the electrochemical sensor will compare the defined threshold for the first pulse with the maximum concentration measured in the next pulse and we named it as comparator rate, $\hat{r}_{r,g}$. If the result lies below 0.5 (to be closer to the standard detector threshold value), the electrochemical sensor adjusts the blind detector threshold; otherwise, it maintains the previous threshold value. We describe this process as follows

$$\hat{r}_{r,g} = \frac{\hat{r}_{u,g,p}}{\max(y_g(z_{2,g}, t_{p+1}))}, \tag{9}$$

where $r = \{1, ..., p_{tot} - 1\}$ is the comparator rate index, and t_{p+1} is the duration of the next pulse. By using the value of the comparator rate, the electrochemical sensor would define whether the threshold should be adjusted or not. Therefore,

$$\begin{cases} \hat{r}_{r,g} & < 0.5, \ \hat{r}_{u,g,p} \text{ will be increased} \\ \hat{r}_{r,g} & \geq 0.5, \ \hat{r}_{u,g,p} \text{ will be maintained.} \end{cases} \tag{10}$$

This adjustment process will take place for every new pulse arriving at the receiver and it is described as follows

$$\hat{r}_{u+1,g,p} = \hat{r}_{u,g,p} + \hat{r}_{u,g,p} * 0.5. \tag{11}$$

C. RLC Probability

Uncertainties, noises and delays, affecting the signal produced by the bacterial populations might result in the incorrect detection of the emitted pulses by the electrochemical sensors. In typical communications systems, the probability of error is often used to evaluate the impact caused by these uncertainties and considered as a performance metric [11], [19]. Here we quantify the accuracy of the BMCoC molecular computations by investigating the probability of obtaining correct values from the detection. To measure the reliable logic computation probability (RLC) of the BMCoC, we first sampled a received signal to evaluate the number of "0's" and "1's" that are correctly detected. The digitalisation process is defined as follows: the molecular output signal is divided in j_{tot} samples and each one of them is compared against the receiver threshold; when the sample is higher than the threshold we associate a logical value "1", otherwise we associate the logical value "0". Please note this notation is true for any threshold values used by the receiver (either fixed or variable). Mathematically, this is described as follows

$$\begin{cases} y_g(z_{2,g}, t) \geq \hat{r}_{std,g}, \ y_g[j] = 1 \\ y_g(z_{2,g}, t) < \hat{r}_{std,g}, \ y_g[j] = 0 \\ y_g(z_{2,g}, t) \geq \hat{r}_{u,g,p}, \ y_g[j] = 1 \\ y_g(z_{2,g}, t) < \hat{r}_{u,g,p}, \ y_g[j] = 0, \end{cases} \tag{12}$$

where each pulse is composed of 50 samples (j) and $j_{tot} = 500$ is the total number of samples. Based on the digital representation of the molecular output signal, we define the reliable logic computation RLC as the measurement of the number of correct detections performed by the electrochemical sensor. In other words, we can compute how many "0's" and "1's" are correctly defined (true negatives - TN, and true positives - TP, respectively) in relation to the total number of samples of the molecular output signal. Therefore, we describe the probability of reliable logic computation as

$$RLC(\%) = \frac{TP + TN}{j_{tot}} \times 100. \tag{13}$$

VI. Results

In this section, we present the results from our performance analysis of the BMCoC. First, we introduce the results of the molecular signals production by the engineered bacterial populations, AND gate and ON-OFF switch. Second, we

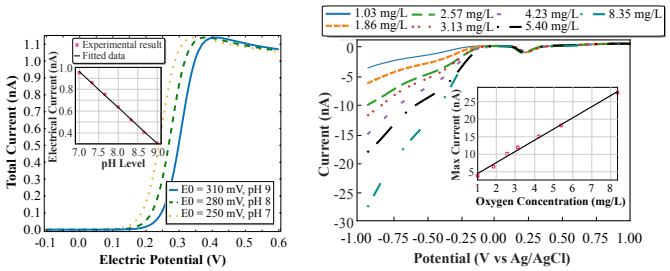

(a) (b)

Fig. 6. Investigation of the operation range for the electrochemical sensors. (a) LARGE: Cyclic voltammograms over the pH range of **7** to **9**. As the pH decreases (as more molecules are generated), a lower redox potential $\boldsymbol{E_0}$ of ferrocene is needed. SMALL: The electrical current values for different pH levels when the electric potential is fixed at $\mathbf{0.28}$ V. The decrease rate was measured as $\mathbf{-32.97}$ mV/pH. The sensitivity of the nanowire sensors [31] means the current value at $\mathbf{0.28}$ V can be used as a probe for the pH change in a solution. (b) LARGE: Cyclic voltammograms of various concentrations (in parts per million) of oxygen at a gold microband array. The cyclic voltammograms were swept from $\mathbf{1.2}$ V to $\mathbf{-0.9}$ V at $\mathbf{50}$ mV/s in water samples at pH $\mathbf{8}$. SMALL: The calibration plot using the current values at $\mathbf{-0.9}$ V versus the measured concentration of oxygen in water.

present the results of the electrochemical sensing process, including the generated electrical current and potential caused by the pH and dissolved oxygen changes. Finally, we present the results of the reliable logic computation probability when using the standard and blind detector thresholds and the molecular communications systems is affected by noises and delays, from the molecular production and propagation.

A. System-Wide Analysis of the BMCoC

1) Implementation of Bacteria Molecular Computing Mechanisms: In the experiment illustrated in Figure 4, we inserted two molecular input signals with the concentrations of 0.1 mmol/L and 0.5 mmol/L into a tube containing the engineered bacterial population representing the AND gate and measured the molecular output signal. Figure 4 (a) shows the results of the possible combinations of molecular input signals, and the different shades of yellow are the output from the AND logic operation. In this case, no colour means low molecular input signals; the light yellow represents the combination of a low and a high molecular input signals, and the darker yellow occurred when adding two high molecular input signals to the tube. As the dark yellow results from the AND gate activation, we quantified the production of the molecular output signal in this scenario for four hours, see Figure 4 (b). Please note that the AND gate's molecular output signal increases almost linearly with time. This result was due to the chosen observation time that occurs before the engineered bacteria started operating in the steady-state regime [38]. Furthermore, this enabled us to observe how quickly the engineered bacterial population could emit the molecular output signal and help us to set up the detector threshold values applied in Section VI-B.

To quantify the operation of the ON-OFF switch, we engineered a bacterial population to use acetate and propionate, with 0.2 mmol/L and 0.4 mmol/L acetate and 0.16 mmol/L and 0.2 mmol/L propionate concentrations (in at least triplicate), respectively. Initial O_2 consumption rates ($\mathrm{mg.O_2.min^{-1}}$) were calculated from the linear portion of the acetate and propionate O_2 consumption response that occurred 10 seconds after (i.e., insertion delay) acetate and propionate were added to the respective acetate and propionate biosensors and presented in Figures 4c. In the case of acetate, the engineered bacteria produced mean O_2 consumption rates of 1.622 and $2.967\,\mathrm{mg.O_2.min^{-1}}$ for respective 0.2 and 0.4 mM acetate concentrations. The standard deviation for both concentrations did not exceed $0.09\,\mathrm{mg.O_2.min^{-1}}$. The propionate biosensor produced 1.8 and $2.350, \mathrm{mg.O_2.min^{-1}}$ for 0.16 and 0.21 mM propionate concentrations. The standard deviation for both concentrations did not exceed $0.038, \mathrm{mg.O_2.min^{-1}}$, see Figure 4c. It is evident from both scenarios that the O_2 consumption rates can be applied as the trigger for the bacteria processing of acetate and propionate concentrations even when subjected to unwanted effects, such as insertion delay.

2) Electrochemical Sensing: We simulate the electrochemical sensor detection process using a finite element software, COMSOL Multiphysics®(version 5.3). For this particular simulation, we considered a microfluidic channel as shown in Figure 5 (see Appendix II for more details).

Due to the small concentration of protons (in the range of nmol/L) produced by the engineered bacterial population, the acidification of the fluid medium will be more sensitive in the pH range of 9 to 7 (from 1 nmol/L to 100 nmol/L). For example, the standard detector threshold for the AND gate operation result in the addition of 2.27×10^{-8} protons to the fluid (or pH 7.64), see Section VI-B.1 for details. By assuming a 1:1 molecular concentration relationship, this threshold value would reduce the pH_f of a fluid as follows

$$\begin{aligned} \mathrm{pH}_f &= -\log_{10}(\mathrm{pH}_9 + \mathrm{pH}_{7.64}) \\ &= -\log_{10}(1 \times 10^{-9} + 2.27 \times 10^{-8}) = 7.62, \end{aligned} \tag{14}$$

and

$$\begin{aligned} \mathrm{pH}_f &= -\log_{10}(\mathrm{pH}_7 + \mathrm{pH}_{7.64}) \\ &= -\log_{10}(100 \times 10^{-9} + 2.27 \times 10^{-8}) = 6.91. \end{aligned} \tag{15}$$

We noted from (14) and (15) that a molecular output signal with the concentration of 2.27×10^{-8}mol/L can produce a greater pH level change if the fluid has a pH 9 than if it had a pH 7. These pH level changes result in the production of different electrical currents when measured at a given electric potential, as shown in Figure 6 (a). A small increase in the pH level results in a significantly different electric current value when measured at a fixed potential of 0.28 V, facilitating the detection of small output molecular signal concentrations.

Based on our previous analysis, we defined an electric potential of 0.28 V to simulate the detection of the molecular output signal by the electrochemical sensors. Through this experiment, we determine the electric current required to oxidate the signalling molecule (FcCOOH). Figure 6 (a) show the result obtained from this analysis. When the fluid channel has a pH of 7, a higher electrical current passes through the electrochemical sensors at the fixed potential than when it has a pH of 9. Therefore, a small ion concentration change, such as 22.7 nmol/L, is harder to be detected for a fluid with a

TABLE I
PARAMETERS CONSIDERED FOR THE THEORETICAL ANALYSIS OF THE BMCOC

Variable	Value	Unit	Reference
K_A, K_B, K_C	10	–	[11]
$z_{1,g}$	5	μm	*
$z_{2,g}$	50	μm	*
r_{ch}	5	μm	*
$h_{ch,1}$	10	μm	*
m_A, m_C	1.2	mmol/L	*
m_B	1.8	mmol/L	*
D	1.37×10^{-7}	m^2/s	[11]
γ	0.01	–	[11]
n	2	–	[11]
t_c	720	seconds	*
t	5	hours	*
t_p	30	minutes	*
τ_{in}, τ_g	100	seconds	*
Γ_s	34.892	–	[38, Ch. 21]
T	300.15	K	*
a_e	100	μm^2	*
k	1.380649×10^{-23}	J/K	[42]

* Value extracted from the experiments by the authors.

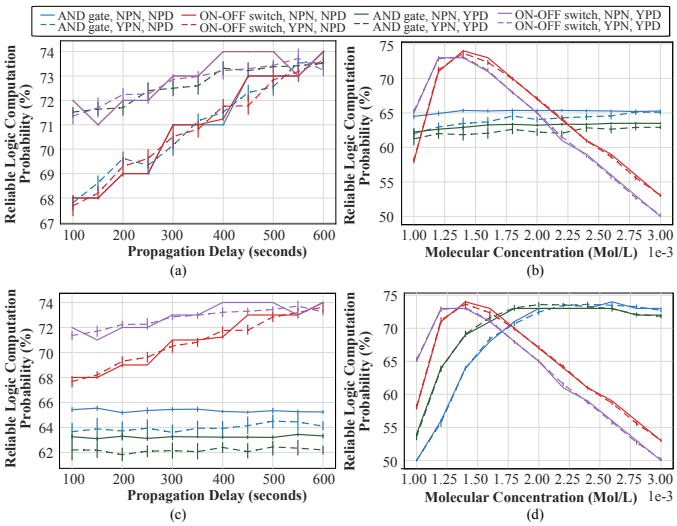

Fig. 7. Reliable logic computation probability for different concentrations of the molecular generated signals. (a) When the system is both affected/not affected by the production and propagation noise, as well as production delay for the AND gate and ON-OFF switch, considering a standard detector threshold. (b) Scenario similar to (a), but considering a range of molecular input concentrations. (c) When the system is both affected/not affected by the production and propagation noise, as well as production delay for the AND gate and ON-OFF switch, considering the blind detector threshold. (d) Scenario similar to (c), but considering a range of molecular input concentrations.

lower pH level. From this result, we also can propose a linear equation to fit the data and predict the electric current for other pH levels, see the small plot in Figure 6 (a), as follows

$$I_c = -0.3219\text{pH}_c + 3.1867, \tag{16}$$

where pH_c is the pH level of the considered fluid media. Using (16), we found that for the defined threshold value (3.2 nM, or pH 8.5), the electrical current produced by the electrochemical sensors was equal to $I_c = 0.45$ nA.

Figure 6 (b) shows the measurement of the dissolved oxygen in water using a gold microband array. This figure shows the cyclicvoltammogram (CV) performed in each concentration of oxygen sweeping from 1.2 V to – 0.8 V vs. Ag/AgCl at 50 mV/s for 3 cycles. The oxidation event at 0.7 V corresponds to the formation of a gold oxide surface layer. The reduction event at 0.25 V corresponds to the reduction of the formed gold oxide layer. These events are independent of oxygen, and the onset of oxygen reduction occurs at -0.1 V in the CV and is characterised as two waves. The first is the reduction of oxygen to hydrogen peroxide, seen at approximately -0.5 V. The second wave is the reduction of the hydrogen peroxide to water, seen at -0.9 V. These waves indicates the complete oxygen reduction, and the electric current measured is linearly dependent on the concentration of oxygen.

3) Countering Unwanted Effects in the Experiments: In Section IV, we consider the effects of delay on our formulation of molecular communications model. Here we describe how we handled the possible unwanted effects that could affect our experimental results.

In electrochemistry assays, we typically evaluate the effects of noise and interference through a background analysis of the obtained results [43]. This type of study enable us to propose specific solutions to the effects caused by molecular delay or interference. For instance, an oxygen permeable membrane will be applied to our BMCoC design to prevent competing reactions. In this case, where we are measuring a change in oxygen concentrations over time, the electrochemical response will increase proportional only to oxygen concentration. An interfering molecule would have a constant current that could easily be background subtracted, and if it is not reactive in this electrochemical window, there may be a change in the capacitance of the solution which would slightly increase background capacitance. As we are using ultra-micro electrodes however, background capacitance is a minimal factor and it may slightly decrease the sensitivity of the sensor, albeit by a negligible amount.

In the case of the microbiology assays, it is possible to counter the molecular noise and interference by using recombinant cell populations that are lab-designed and commercially available that do not produce any other proteins (to a substantial degree), apart from normal essential intercellular proteins for the cell to live and divide. In our experimental setting, the engineered bacterial population will be specialised in the production of the molecular output signal, minimising the effects of interference. In addition to that, there is another (and more important) method to remove biological noise/interference that may affect measurements, which is by including a series of negative controls and subtracting these from the experimental data. For instance, we can add 'blank' samples and subtract their final absolute values from the actual sample experimental data [44]. For our analysis, these 'blank' samples are experiments that contain cells but no substrate

(nitrile) and also cells with substrate but no inducer (IPTG). We also included experiments with both compounds but no cells, in case they are producing some interference. Please note that we have subtracted the 'blank' samples from our experimental results. Regarding the delay in our microbiology assay, we use a high molecular concentration of the substrate, resulting in an immediate triggering of the engineered bacterial population, which will require some time to produce the molecular output signal to a level that is detectable by the spectrophotometer (see Figure 4b) or electrochemical sensor (see Figure 6).

B. RLC for Different Signal Detectors

Our analysis considers that the different molecular input signals inserted into each microfluidic chamber will propagate through the fluid channel (it can suffer a propagation delay τ_{in}) and are detected and processed by the bacteria-based logic gate populations. Here, we apply the molecular computing models introduced in Section IV. Based on these models, we evaluate the reliable logic computation probability when the bacteria-based logic gate processing is instantaneous or delayed by 720 seconds (defined as production delay). We determined the different scenarios as NPN - no production noise, NPD - no production delay, YPN - with production noise, and YPD - with production delay. Moreover, due to the stochastic nature of some processes here investigated, we run each scenario ten times and evaluate the average and standard deviation of these values. For our analysis, we use the values presented in Table I. Additionally, we consider an AWGN noise to model the fluctuation in the production of the molecular signals. This molecular production noise will have an average of $\mu_c = 0$ and variance of $\sigma_{AND} = 2\,\text{nmol/L}$ for the AND gate and $\sigma_{ON} = 1\,\text{nmol/L}$ for the ON-OFF switch. The molecular output signal $y_g(z_{2,g}, t)$ is produced for five hours. The bacteria-based logic gates and the electrochemical sensors have a distance of $d_{TS} = 50\,\mu\text{m}$ between each other. The production and electrolyte noises, as well as the production and propagation delays, will induce errors in the molecular output signal detection. This is due to the incorrect identification of positive and negative samples in the digitalised version of the molecular output signal $y_g(z_{2,g}, t)$. Therefore, we investigate the impact of the delays and noises on this bacteria-based molecular communications system by evaluating the reliability logic computation probability for different scenarios.

1) Standard Detector Threshold Analysis: First, we investigate the electrochemical sensor standard detector threshold to study the probability of the correct detection of the molecular output signal. In this case, we considered the molecular input signals $s_A = s_B = s_C$ as pulse trains, with concentrations equal to $m_A = m_C = 1.2$ mmol/L, and $m_B = 1.8$ mmol/L. By applying these molecular signals in (2)-(7), we are able to evaluate the standard detector threshold as $\hat{r}_{std,AND} = 2.27 \times 10^{-8}$ mol/L for the AND gate and $\hat{r}_{std,ON} = 1.01 \times 10^{-8}$ mol/L for the ON-OFF switch. We apply these standard detector thresholds in (12), evaluate the number of positive and negative samples and compare it with the molecular input signals for a varying propagation delay. Figure 7 (a) shows the logic computation reliability for this case, and it can be noted that the AND gate is impacted more by the uncertainties of these bacteria-based communications systems than the ON-OFF switch. It can also be noted that the AND gate has a higher reliability than the ON-OFF switch for most values of propagation delay. Furthermore, as we increase the propagation delay from 100 to 600 seconds, the reliability logic computation probability for both AND and ON-OFF switch improves, which allow us to induce that the propagation delay counter the effect of the system's uncertainties.

Next, we evaluated the reliable logic computation probability, considering a fixed propagation delay of 100 seconds and different molecular input signals concentration m_B and m_C (ranging from 1μmol/L to 3μmol/L), which is shown in Figure 7 (b). In this scenario, the ON-OFF switch dramatically decrease its performance if more molecular signal is input into the system, with the no production delay cases performing better than the cases where the production delay was considered. Therefore, for minimal effects on the overall performance of this gate, only a small range of molecular input signal can be considered (from 1.12 mmol/L to 1.60 mmol/L). Figure 7 (b) also shows that the AND gate reliable logic computation probability reaches a plateau for molecular input signal concentrations above 1.75 mmol/L for the no production delay case and 2 mmol/L when there is delay on the production of the molecular output signal. These results shows that the logic computation using AND gates is more robust against a wide range of molecular input signal concentrations, but it can suffer considerably for lower difference between the production and propagation delays. On the other hand, the ON-OFF switch tends to be more robust against the delay difference and for a small range of molecular input signal concentrations.

2) Blind Detector Threshold Analysis: We also evaluate the reliable logic computation probability considering the blind detector threshold defined in (8)-(10) and the same scenarios of the standard detector threshold (see Section VI-B.1). Figure 7 (c) shows the scenario where different propagation delay values are considered. For both gates, AND gate does not have its reliable logic computation probability affected by the propagation delay. This result is due to the different detection process, which is more robust to the possible variations caused by the propagation delay. Despite that, this same technique is not robust enough for the ON-OFF switch, which improves its reliability when considering higher propagation delays. When comparing the reliable logic computation probability of the ON-OFF switch depicted in Figures 7 (a) and 7 (c), one can note that they are similar, which shows this specific gate can use both detector thresholds without affecting the BMCoC's performance.

Following the propagation delay analysis, we investigate the impact of the different molecular input signal concentrations m_B and m_C (the same values applied for the standard detector threshold analysis) on the reliability of logic computation of both gates, when considering the blind detector threshold, see Figure 7 (d). In this scenario, the AND gate shows a different performance when compared with the standard

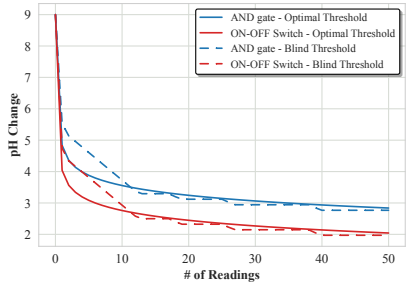

Fig. 8. Evaluation of the pH change saturation due to the cumulative addition of the molecular signal produced by the engineered bacteria on the fluid media around the electrochemical sensor for the AND gate and ON-OFF switch after multiple readings, for both proposed detection thresholds.

detector threshold. The molecular input signal concentrations considered in this analysis are in the plateau range of the AND gate, which happen for values above 1.75 mmol/L for Figure 7 (b). On the other hand, the ON-OFF switch has high reliability for a small range of molecular input signal concentrations with a range of 1.12 mmol/L to 1.60 mmol/L. Therefore, the ON-OFF switch performance shows the same behaviour for both scenarios when comparing Figures 7 (b) and 7 (d). These results showed that the blind detector threshold gave stability for the digitalisation process of the molecular output signal produced by the AND gate and did not affect the performance of the molecular output signal detection originated from the ON-OFF switch.

3) Saturation: The number of readings that the sensor can perform before losing its sensitivity is an essential parameter for the proposed BMCoC system. Therefore, based on the results obtained by the electrochemical sensor detection thresholds analysis, we can evaluate this limit for the pH variation detection. For example, by adding 2.27×10^{-8} protons, we would change the pH of fluid from 9 to 7.62. If repeating this process one more time, the pH would reduce from 7.62 to 7.33. By repeating this process several times, the pH reduction will become so small that it becomes hard to be detected by the electrochemical sensor. Therefore, we evaluate this saturation of the electrochemical sensor for the cumulative molecular output signal concentration as shown in Figure 8. Both the standard and blind detector thresholds shows an exponential-like decrease for the pH variation, as this saturation model follows the same calculations from (14)-(15). However, the standard detector threshold has a smoother curve than the blind detector threshold. Moreover, despite showing a more abrupt pH reduction for the initial 12 readings, the blind threshold showed a similar pH reduction for the remaining measurements. This result suggests that even electrochemical sensors with lower sensitivity (only detect high pH variations) can use the blind detector threshold.

VII. Conclusion

In this paper, we introduced the experimental and theoretical analysis of a Bacterial Molecular Computing on a Chip that contains engineered cells performing computation based on input molecular signals. The molecular signal output from the engineered bacterial population modifies the pH or the dissolved oxygen concentration, which is sensed by the electrochemical sensors used for detection. The paper also investigated the computation reliability of the BMCoC under the impact of unwanted effects, i.e., molecular production and propagation delays, as well as electrolyte noise. Our experimental analysis showed the engineered bacterial population's ability to detect molecular signals (e.g., acetate and propionate) at low concentrations and can produce required output to be detected by the electrochemical sensors. Furthermore, the electrochemical sensors showed a linear dependency on the pH and dissolved oxygen concentration variation, granting certain robustness to these sensors. We also found that considering a detection threshold of 2.27×10^{-8} mol/L (or pH 7.64), the electrochemical sensors can operate better if the fluid medium has a pH 9 instead of a pH 7. This threshold result into a minimal electrical current level ($I_c = 0.45$ nA) for the molecular output signal concentration detection. We also show that the AND gate have a more robust logic computation performance than the ON-OFF switch for the analysed scenarios. However, the ON-OFF switch could achieve a higher reliable logic computation probability than the AND gate for these same scenarios. The BMCoC can open up to a plethora of different diagnostic applications, and can lay the foundation for the development of future Internet of Bio-Nano Things.

Appendix I
Engineered Bacteria

We designed a wet lab experiment where a AND gate process nitrile and IPTG molecular concentrations to output ammonia and hydrogen, that would change the pH of the media around the electrochemical sensors. The detection of AND logic operation can be done by measuring the ammonia (spectroscopy) or the hydrogen ions (pH variation). In this experiment, we investigate ammonia production by using Nessler's microscale ammonia assay [45]. Assays were carried out in 150 μL format containing potassium phosphate buffer pH 7, a final cell O.D. @600 nm of 0.5 and a final substrate (nitrile) concentration of 0 mmol/L, 5 mmol/L or 10 mmol/L (no, low or high molecular output signal amplitude, respectively). The amounts of enzyme expression inducer, IPTG (Isopropyl-β-D-thiogalactopyranoside, Zymo Research, L1001-5), was either 0 mmol/L, 0.1 mmol/L or 0.5 mmol/L (no, low or high IPTG, respectively) to test the operation of the AND logic gate. The reaction was carried out over 5 hours with regular readings taken throughout. To quench the continued generation of signal, 37.5 μL of 250 mmol/L HCl (Sigma-Aldrich, Cat. No. 435570) was added to stop the reaction. Cell biomass was removed at 500 x g for 10 minutes at 4 °C to be able to quantify the molecular output concentration. We transferred 20 μL of the quenched reaction supernatant to a microtiter plate and to this 181 μL of the Nessler's master mix was added (151 μL deionised H_2O, 1.0 μL 10N NaOH (Sigma-Aldrich, Cat. No. 765429) and 25 μL Nessler's reagent (Sigma-Aldrich, 72190). The reaction supernatant was incubated at room temperature (22 °C) for 10 minutes and the absorbance was read at 425 nm.

A nitrilase gene from a *Burkholderia* bacteria was PCR amplified and cloned to an expression vector to process

molecules as an AND logic gate. Each $15\,\mu$L PCR reaction mixture contained $7.5\,\mu$L Platinum™SuperFi™Green PCR Master Mix (ThermoFisher Scientific, Cat. No. 12359010), $15\,\mu$M of each primer and $1\,\mu$L cell suspension with a final cell O.D. @$600\,$nm $= 0.04$. The following PCR conditions were used: 1 cycle of $95\,^{\circ}$C for 5 min, 30 cycles of $95\,^{\circ}$C for 1 min, $56\,^{\circ}$C for 1 min, $72\,^{\circ}$C for 2 min, followed by 1 cycle of $72\,^{\circ}$C for 5 min. The PCR product was cleaned using the Zymo Research clean and concentrator™-5 (Zymo Research, Cat. No. D4013) as per the manufacturer instructions with elution in water. The pRSF-2 Ek/LIC vector (Novagen, Cat. No. 71364) was used for expression of the nitrilase. Cloning procedures were followed as per manufacturer's instructions, with ligations transformed to E. coli BL21 (DE3) as per manufacturer's guidelines for heat shock transformations.

For the ON-OFF switch, the bacterial population was created by cultivating, extracting and immobilizing acetate and propionate grown A11 and P1 cells, respectively. This engineering process is similar to the methods previously described by [46], however, the following modifications were made for this study: 1.) The IMD Wldgyep (acetate biosensor) strain was renamed A11, while the IMD Wldgyepak (propionate biosensor) strain was replaced with P1 cells which differ in that their ability to catabolise formate has been removed; 2.) The previously used dissolved oxygen (DO) probe was updated with an array of Vernier (DO-BTA) DO probes. These probes were selected due to their affordability, their increased sampling frequency (1 Hz) and their ability to be interfaced as an array using Arduino microcontrollers. For Vernier DO probes to be made compatible with the previously developed cell immobilization technique, Vernier probe tips needed to be modified slightly. Vernier DO probe tips are concave in shape which results in their oxygen permeable membranes being exposed. To project the membrane, Vernier probe tips possess raised bevel rings. Immobilized cells can only be fixed to a smooth probe tip surface and as such Vernier's protective bevels had to be removed by a scalpel. To ensure that fixed cells are protected from magnetic stirrer flea impacts in the absence of raised levels, perforated steel guards were fabricated and fitted on top of the cells.

Appendix II
Electrochemical Sensors

The pH change will be detected by the electrochemical sensors measuring the oxidation/reduction potentials of a signalling mediator molecule. A similar process was applied by Wahl et. al to simulate the electric current on a gold nanowire electrode [47]. Furthermore, we use *ferrocene monocarboxylic acid* (FcCOOH), a signalling molecule, to detect the production of protons (in this case, H^+) and the consequent decrease in pH [47], [48]. The redox potential E_0 of FcOOH has a pH dependence of $+30$mV/pH at a polypyrrole modified reference electrode [47]. FcCOOH at a polypyrrole reference electrode has a higher redox potential for high pH levels, meaning that when more protons are present, a smaller electric potential is required for oxidisation.

Electrochemical oxygen reduction was monitored in samples of water. Each water sample was initially saturated with oxygen, approximately between 8 and 9 ppm of oxygen. This was done by exposing the samples to air at room temperature (17 ∘C), typically overnight. To decrease the concentration of oxygen, water samples were purged by bubbling nitrogen into the sample for 30 minutes. After purging, the water samples were covered with parafilm to keep the oxygen from dissolving back into the solution. This sample was measured as the lowest oxygen concentration, which typically contained less than 1 ppm. The parafilm was perforated after the first oxygen measurement to allow oxygen to dissolve back into the solution gradually. It was found that oxygen typically re-dissolved at different rates depending on the solution concentration. Rates of 1 ppm per 3 minutes were observed when the concentration was between 0 and 4 ppm. From 4 - 6 ppm, a rate of 1 ppm per 7 minutes was observed. To increase the oxygen concentration beyond 6 ppm, the solution, the solution was bubbled with oxygen, as the time to reach saturation by diffusion was considerably longer. Typical calibrations using this method were with concentrations between fully purged (0.5 ppm), and fully saturated (8.8 ppm). All oxygen concentrations were measured using a commercial optical DO probe (Hach, LDO101). The electrochemical analysis was carried out using an Autolab potentiostat, with the electrochemical cell kept in a Faraday cage. A gold-gold IDE array was used for this work.

References

[1] A. Goñi-Moreno and P. I. Nikel, "High-performance biocomputing in synthetic biology–integrated transcriptional and metabolic circuits," *Frontiers in Bioengineering and Biotechnology*, vol. 7, p. 40, 2019.

[2] J. M. Jornet, Y. Bae, C. R. Handelmann, B. Decker, A. Balcerak, A. Sangwan, P. Miao, A. Desai, L. Feng, E. K. Stachowiak *et al.*, "Optogenomic interfaces: Bridging biological networks with the electronic digital world," *Proceedings of the IEEE*, vol. 107, no. 7, pp. 1387–1401, 2019.

[3] M. Bartunik, M. Fleischer, W. Haselmayr, and J. Kirchner, "Advanced characterisation of a sensor system for droplet-based microfluidics," in *2020 IEEE SENSORS*. IEEE, 2020, pp. 1–4.

[4] M. Kuscu, E. Dinc, B. A. Bilgin, H. Ramezani, and O. B. Akan, "Transmitter and receiver architectures for molecular communications: A survey on physical design with modulation, coding, and detection techniques," *Proceedings of the IEEE*, vol. 107, no. 7, pp. 1302–1341, 2019.

[5] C.-Y. Hsu, B.-K. Chen, R.-H. Hu, and B.-S. Chen, "Systematic design of a quorum sensing-based biosensor for enhanced detection of metal ion in escherichia coli," *IEEE Transactions on Biomedical Circuits and Systems*, vol. 10, no. 3, pp. 593–601, 2016.

[6] P. Mehta, S. Goyal, T. Long, B. L. Bassler, and N. S. Wingreen, "Information processing and signal integration in bacterial quorum sensing," *Molecular Systems Biology*, vol. 5, no. 1, p. 325, 2009.

[7] K. Stephens and W. E. Bentley, "Synthetic biology for manipulating quorum sensing in microbial consortia," *Trends in microbiology*, vol. 28, no. 8, pp. 633–643, 2020.

[8] M. O. Din, A. Martin, I. Razinkov, N. Csicsery, and J. Hasty, "Interfacing gene circuits with microelectronics through engineered population dynamics," *Science Advances*, vol. 6, no. 21, p. eaaz8344, 2020.

[9] J. Shin, S. Zhang, B. S. Der, A. A. Nielsen, and C. A. Voigt, "Programming escherichia coli to function as a digital display," *Molecular systems biology*, vol. 16, no. 3, p. e9401, 2020.

[10] A. A. Green, J. Kim, D. Ma, P. A. Silver, J. J. Collins, and P. Yin, "Complex cellular logic computation using ribocomputing devices," *Nature*, vol. 548, no. 7665, pp. 117–121, 2017.

[11] D. P. Martins, M. T. Barros, and S. Balasubramaniam, "Quality and capacity analysis of molecular communications in bacterial synthetic logic circuits," *IEEE Transactions on NanoBioscience*, vol. 18, no. 4, pp. 628–639, 2019.

[12] N. A. Abbasi and O. B. Akan, "An information theoretical analysis of human insulin-glucose system toward the internet of bio-nano things," *IEEE Transactions on NanoBioscience*, vol. 16, no. 8, pp. 783–791, 2017.

[13] I. F. Akyildiz, M. Pierobon, and S. Balasubramaniam, "Moving forward with molecular communication: From theory to human health applications [point of view]," *Proceedings of the IEEE*, vol. 107, no. 5, pp. 858–865, 2019.

[14] D. Bi, A. Almpanis, A. Noel, Y. Deng, and R. Schober, "A survey of molecular communication in cell biology: Establishing a new hierarchy for interdisciplinary applications," *IEEE Communications Surveys & Tutorials*, 2021.

[15] I. F. Akyildiz, M. Pierobon, and S. Balasubramaniam, "An information theoretic framework to analyze molecular communication systems based on statistical mechanics," *Proceedings of the IEEE*, vol. 107, no. 7, pp. 1230–1255, 2019.

[16] B. D. Unluturk, S. Balasubramaniam, and I. F. Akyildiz, "The impact of social behavior on the attenuation and delay of bacterial nanonetworks," *IEEE transactions on nanobioscience*, vol. 15, no. 8, pp. 959–969, 2016.

[17] M. T. Barros, S. Balasubramaniam, B. Jennings, and Y. Koucheryavy, "Transmission protocols for calcium-signaling-based molecular communications in deformable cellular tissue," *IEEE Transactions on Nanotechnology*, vol. 13, no. 4, pp. 779–788, 2014.

[18] M. T. Barros, P. Doan, M. Kandhavelu, B. Jennings, and S. Balasubramaniam, "Engineering calcium signaling of astrocytes for neural–molecular computing logic gates," *Scientific reports*, vol. 11, no. 1, pp. 1–10, 2021.

[19] M. Pierobon and I. F. Akyildiz, "Diffusion-based noise analysis for molecular communication in nanonetworks," *IEEE Transactions on Signal Processing*, vol. 59, no. 6, pp. 2532–2547, 2011.

[20] T. Plesa, K. C. Zygalakis, D. F. Anderson, and R. Erban, "Noise control for molecular computing," *Journal of The Royal Society Interface*, vol. 15, no. 144, p. 20180199, 2018.

[21] N. Khalid, I. Kobayashi, and M. Nakajima, "Recent lab-on-chip developments for novel drug discovery," *Wiley Interdisciplinary Reviews: Systems Biology and Medicine*, vol. 9, no. 4, p. e1381, 2017.

[22] E. Valera, J. Berger, U. Hassan, T. Ghonge, J. Liu, M. Rappleye, J. Winter, D. Abboud, Z. Haidry, R. Healey *et al.*, "A microfluidic biochip platform for electrical quantification of proteins," *Lab on a Chip*, vol. 18, no. 10, pp. 1461–1470, 2018.

[23] D. Lombardi and P. S. Dittrich, "Droplet microfluidics with magnetic beads: A new tool to investigate drug–protein interactions," *Analytical and bioanalytical chemistry*, vol. 399, no. 1, pp. 347–352, 2011.

[24] S. Dudala, S. K. Dubey, and S. Goel, "Fully integrated, automated, and smartphone enabled point-of-source portable platform with microfluidic device for nitrite detection," *IEEE Transactions on Biomedical Circuits and Systems*, vol. 13, no. 6, pp. 1518–1524, 2019.

[25] Y. Zhao and K. Chakrabarty, "Digital microfluidic logic gates and their application to built-in self-test of lab-on-chip," *IEEE Transactions on Biomedical Circuits and Systems*, vol. 4, no. 4, pp. 250–262, 2010.

[26] K. Yagi, "Applications of whole-cell bacterial sensors in biotechnology and environmental science," *Applied Microbiology and Biotechnology*, vol. 73, no. 6, pp. 1251–1258, 2007.

[27] N. Farsad, A. W. Eckford, S. Hiyama, and Y. Moritani, "On-chip molecular communication: Analysis and design," *IEEE Transactions on NanoBioscience*, vol. 11, no. 3, pp. 304–314, 2012.

[28] L. Grebenstein, J. Kirchner, W. Wicke, A. Ahmadzadeh, V. Jamali, G. Fischer, R. Weigel, A. Burkovski, and R. Schober, "A molecular communication testbed based on proton pumping bacteria: Methods and data," *IEEE Transactions on Molecular, Biological and Multi-Scale Communications*, vol. 5, no. 1, pp. 56–62, 2019.

[29] A. M. Zoubir, V. Koivunen, Y. Chakhchoukh, and M. Muma, "Robust estimation in signal processing: A tutorial-style treatment of fundamental concepts," *IEEE Signal Processing Magazine*, vol. 29, no. 4, pp. 61–80, 2012.

[30] S. Hiyama, Y. Moritani, and T. Suda, "Molecular transport system in molecular communication," *NTT DOCOMO Technical Journal*, vol. 10, no. 3, pp. 49–53, 2008.

[31] K. Dawson, A. Wahl, S. Barry, C. Barrett, N. Sassiat, A. J. Quinn, and A. O'Riordan, "Fully integrated on-chip nano-electrochemical devices for electroanalytical applications," *Electrochimica Acta*, vol. 115, pp. 239–246, 2014.

[32] J.-u. Shim, S. N. Patil, J. T. Hodgkinson, S. D. Bowden, D. R. Spring, M. Welch, W. T. Huck, F. Hollfelder, and C. Abell, "Controlling the contents of microdroplets by exploiting the permeability of pdms," *Lab on a Chip*, vol. 11, no. 6, pp. 1132–1137, 2011.

[33] K. Dawson, A. Wahl, R. Murphy, and A. O'Riordan, "Electroanalysis at single gold nanowire electrodes," *The Journal of Physical Chemistry C*, vol. 116, no. 27, pp. 14 665–14 673, 2012.

[34] S. Barry, K. Dawson, E. Correa, R. Goodacre, and A. O'Riordan, "Highly sensitive detection of nitroaromatic explosives at discrete nanowire arrays," *Faraday Discussions*, vol. 164, pp. 283–293, 2013.

[35] I. Llatser, D. Demiray, A. Cabellos-Aparicio, D. T. Altilar, and E. Alarcón, "N3sim: Simulation framework for diffusion-based molecular communication nanonetworks," *Simulation Modelling Practice and Theory*, vol. 42, pp. 210–222, 2014.

[36] O. B. Akan, H. Ramezani, T. Khan, N. A. Abbasi, and M. Kuscu, "Fundamentals of molecular information and communication science," *Proceedings of the IEEE*, vol. 105, no. 2, pp. 306–318, 2017.

[37] D. P. Martins, K. Leetanasaksakul, M. T. Barros, A. Thamchaipenet, W. Donnelly, and S. Balasubramaniam, "Molecular communications pulse-based jamming model for bacterial biofilm suppression," *IEEE Transactions on NanoBioscience*, vol. 17, no. 4, pp. 533–542, 2018.

[38] P. Atkins and J. de Paula, *Physical Chemistry*, 8th ed. United Kingdom: Oxford University Press, 2006.

[39] M. J. Deen, M. W. Shinwari, J. C. Ranuárez, and D. Landheer, "Noise considerations in field-effect biosensors," *Journal of Applied Physics*, vol. 100, no. 7, p. 074703, 2006.

[40] A. Akkaya, H. B. Yilmaz, C.-B. Chae, and T. Tugcu, "Effect of receptor density and size on signal reception in molecular communication via diffusion with an absorbing receiver," *IEEE Communications Letters*, vol. 19, no. 2, pp. 155–158, 2014.

[41] M. T. Dabiri and S. M. S. Sadough, "Generalized blind detection of ook modulation for free-space optical communication," *IEEE Communications Letters*, vol. 21, no. 10, pp. 2170–2173, 2017.

[42] T. I. B. of Weights and Measures, *The International System of Units (SI)*, 9th ed. France: The International Bureau of Weights and Measures, 2019.

[43] B.-C. Lai, J.-G. Wu, and S.-C. Luo, "Revisiting background signals and the electrochemical windows of au, pt, and gc electrodes in biological buffers," *ACS Applied Energy Materials*, vol. 2, no. 9, pp. 6808–6816, 2019.

[44] S. Ikeno and T. Haruyama, "Boost protein expression through co-expression of lea-like peptide in escherichia coli," *PLoS One*, vol. 8, no. 12, p. e82824, 2013.

[45] T. M. Coady, L. V. Coffey, C. O'Reilly, E. B. Owens, and C. M. Lennon, "A high throughput screening strategy for the assessment of nitrile-hydrolyzing activity towards the production of enantiopure β-hydroxy acids," *Journal of Molecular Catalysis B: Enzymatic*, vol. 97, pp. 150–155, 2013.

[46] J. B. Sweeney, C. D. Murphy, and K. McDonnell, "Development of a bacterial propionate-biosensor for anaerobic digestion monitoring," *Enzyme and Microbial Technology*, vol. 109, pp. 51–57, 2018.

[47] A. Wahl, S. Barry, K. Dawson, J. MacHale, A. J. Quinn, and A. O'Riordan, "Electroanalysis at ultramicro and nanoscale electrodes: A comparative study," *Journal of The Electrochemical Society*, vol. 161, no. 2, pp. B3055–B3060, Dec 2014.

[48] R. Raoof, Jahan-Bakhshand Ojani and F. Chekin, "Electrochemical analysis ofd-penicillamine using a carbon paste electrode modified with ferrocene carboxylic acid," *Electroanalysis*, vol. 19, no. 18, pp. 1883–1889, 2007.

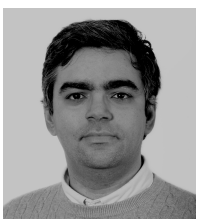

Daniel P. Martins (STM'05, M'19) received his PhD from the Waterford Institute of Technology, Ireland, in 2019. Currently, he is a Postdoctoral Researcher in the Emerging Networks Laboratory at Walton Institute, Ireland.

His research concentrates on the modeling and analysis of conventional and nanoscale communications systems using engineered bacterial populations.

Michael Taynnan Barros is an Assistant Professor (Lecturer) since June 2020 in the School of Computer Science and Electronic Engineering at the University of Essex, UK. He is also a MSCA-IF Research Fellow (part-time) at the Tampere University, Finland. He received the PhD in Computer Science at the Waterford Institute of Technology in 2016. He has over 70 research peer-reviewed scientific publications in top journals and conferences such as Nature Scientific Reports, IEEE Transactions on Communications, IEEE Transactions on Vehicular Technology, in the areas of molecular and unconventional communications, biomedical engineering, bionano science and Beyond 5G. Since 2020, he is a review editor for the Frontiers in Communications and Networks journal in the area of unconventional communications. He also served as guest editor for the IEEE Transactions on Molecular, Biological and Multi-Scale Communications and Digital Communications Networks journals. He received the CONNECT Prof. Tom Brazil Excellence in Research Award in 2020. Dr Barros current research interests include molecular communications, Biocomputing, Internet of Bio-NanoThings and 6G.

Benjamin J. O'Sullivan received a B.S. degree in Chemistry with Forensice Science from University College Cork, Ireland, in 2015. He is currently pursuing a PhD degree at Tyndall National Institute, Cork, Ireland.

His research interests include the development of finite element models, local pH control for electroanalysis and the development of microfluidic electrochemical sensors.

Ian Seymour received the Ph.D. degree in Engineering Science from University College Cork in 2020. He is currently a Post Doctorate researcher in Tyndall National Institute, Cork, Ireland. His current research focuses on the use of dual electrode devices for the development of reagent free, interference free point of care electrochemical sensors.

His research interests include electrochemical nano and ultramicro materials for the development of environment sensor technologies.

Alan O'Riordan received the PhD degree from University College Cork in 2005. He is currently a Senior Research Fellow with the Tyndall National Institute and also a Principal Investigator for Smart Agri-food and Nanosensors and Systems. He coordinates/partners in a portifolio of National and EU projects.

His research interests include nanomaterials and nanofabrication to develop end-to-end highly functional smart sensor system, based on Ram spectroscopy and nanoelectrochemistry.

Lee Coffey was born in Waterford, Ireland and received the BSc. (Hons) degree in Applied Biology with Quality Management from Waterford Institute of Technology (WIT) in 2002. He gained experience in pharmaceutical and food microbiology industrial laboratory roles, before commencing a PhD in Molecular Biotechnology which he completed in 2007 via an IRC(SET) scholarship. From 2007 to 2013, he was a Postdoctoral Researcher and the Molecular Biology Research Lab Manager in the Pharmaceutical & Molecular Biotechnology Research Centre in WIT. From 2005 he was also a part-time lecturer and moved to a full-time lecturer role in WIT in 2013. He is the Principal Investigator of the Molecular Biotechnology & Biopharmaceutical Research Group and is author of 22 publications and numerous inventions, with 5 patents pending across multiple territories currently. He is/has supervised thirteen PhD candidates and postdoctoral researchers to date. He has attracted over €1.7 million research funding to date including Enterprise Ireland and Science Foundation Ireland funding, and has licensed over 1400 biological research technologies to global multi-€B companies. He is the CEO and founder of a spin-out company BIOENZ Technologies Ltd. which has exclusively licensed approx. 4000 biological research technologies and inventions. His research interests include the use of molecular biology techniques to; discover and enhance biopharmaceutical proteins, including gene screening, expression, genome editing, synthetic biology, directed evolution; industrial enzymes for food/feed/pharma/health/industrial applications; biological molecular communications for DNA data storage and biological health monitoring. He was a National Forum Teaching Hero Award Recipient in 2021 and 2020, has been nominated for the 2021 WIT Research Excellence Awards – Established Researcher Category, has been co-awarded the Technology Ireland Awards 2019 – Outstanding Academic Achievement of the Year and also won the WIT Postgraduate Supervision Excellence Award in 2016

Joseph B. Sweeney is from Dublin, Ireland. He receieved a BSc in industrial microbiology in 2007, a MSc in Computer Science in 2012 and a PhD in Biosystems Engineering in 2016, from University College Dublin. From 2016 to 2019, he was a posdoctoral researcher in University College Dublin where he combined his background in computer science and microbiology, to develop E. coli based biosnesors for anaerobic digestors. Since 2019 he has been employed as a Research Fellow in University College Dublin on a project called LIFE farm4more, where he is developing biosensor based monitoring and control solutions for grass-silage fed green biorefineries.

Sasitharan Balasubramaniam received his PhD from University of Queensland, Australia, in 2005. Currently, he is an Associate Professor at the Department of Computer Science and Engineering, University of Nebraska-Lincoln, USA. He was a past PI for SFI VistaMilk and CONNECT research centres in Ireland, and a past Academy of Finland Research Fellow at Tampere University, Finland. His research interests includes molecular communications modeling and simulations and the Internet of Bio-Nano Things. He is currently an Associate Editor for IEEE Transactions on Mobile Computing and IEEE Transactions on Molecular, Biological, and Multi-scale Communications. He is also an Technical Editor for IEEE Academy for IoT, and a past Associate Editor for IEEE Internet of Things journal. In 2018 he was the IEEE Distinguished Lecturer for the Nanotechnology Council.